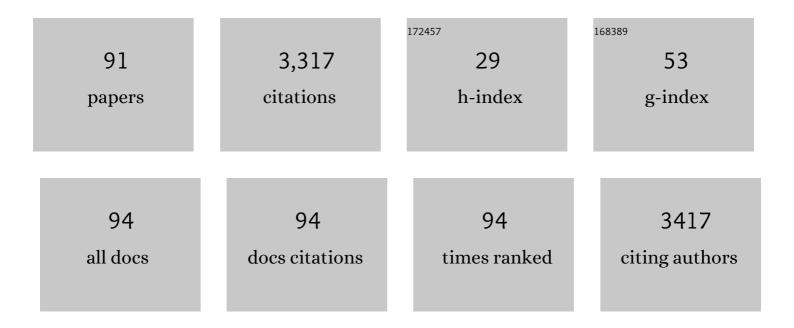
List of Publications by Year in descending order

Source: https://exaly.com/author-pdf/4896594/publications.pdf Version: 2024-02-01



#	Article	IF	CITATIONS
1	An Investigation of Chemoâ€Mechanical Phenomena and Li Metal Penetration in Allâ€Solidâ€State Lithium Metal Batteries Using In Situ Optical Curvature Measurements. Advanced Energy Materials, 2022, 12, .	19.5	24
2	Solid‣tate Li–Metal Batteries: Challenges and Horizons of Oxide and Sulfide Solid Electrolytes and Their Interfaces. Advanced Energy Materials, 2021, 11, .	19.5	312
3	Lithium-film ceramics for solid-state lithionic devices. Nature Reviews Materials, 2021, 6, 313-331.	48.7	80
4	Processing thin but robust electrolytes for solid-state batteries. Nature Energy, 2021, 6, 227-239.	39.5	328
5	Solid State Batteries: Solidâ€State Li–Metal Batteries: Challenges and Horizons of Oxide and Sulfide Solid Electrolytes and Their Interfaces (Adv. Energy Mater. 1/2021). Advanced Energy Materials, 2021, 11, 2170002.	19.5	8
6	All ceramic cathode composite design and manufacturing towards low interfacial resistance for garnet-based solid-state lithium batteries. Energy and Environmental Science, 2020, 13, 4930-4945.	30.8	108
7	Toward Controlling Filament Size and Location for Resistive Switches via Nanoparticle Exsolution at Oxide Interfaces. Small, 2020, 16, e2003224.	10.0	27
8	High energy and long cycles. Nature Energy, 2020, 5, 278-279.	39.5	12
9	Lithiumâ€Battery Anode Gains Additional Functionality for Neuromorphic Computing through Metal–Insulator Phase Separation. Advanced Materials, 2020, 32, e1907465.	21.0	43
10	La _{0.6} Sr _{0.4} Cr _{0.8} Co _{0.2} O ₃ Perovskite Decorated with Exsolved Co Nanoparticles for Stable CO ₂ Splitting and Syngas Production. ACS Applied Energy Materials, 2020, 3, 4569-4579.	5.1	41
11	Facet-Dependent <i>in Situ</i> Growth of Nanoparticles in Epitaxial Thin Films: The Role of Interfacial Energy. Journal of the American Chemical Society, 2019, 141, 7509-7517.	13.7	89
12	Lattice strain-enhanced exsolution of nanoparticles in thin films. Nature Communications, 2019, 10, 1471.	12.8	114
13	High-throughput roll-to-roll fabrication of flexible thermochromic coatings for smart windows with VO ₂ nanoparticles. Journal of Materials Chemistry C, 2018, 6, 3451-3458.	5.5	29
14	Er0.4Bi1.6O3â~'δ– La0.8Sr0.2MnO3â^'δ nano-composite as a low-temperature firing cathode of solid oxide fuel cell. Journal of Power Sources, 2017, 344, 218-222.	7.8	19
15	Thermal cycling and electrochemical characteristics of solid oxide fuel cell supported on stainless steel with a new 3-phase composite anode. Journal of Power Sources, 2017, 354, 74-84.	7.8	17
16	Electrical conductivity of RF-sputtered Gd-doped ceria film measured in across-plane mode. Solid State Ionics, 2017, 309, 58-62.	2.7	4
17	Oxidation of porous stainless-steel coated with donor-doped SrTiO3 in anodic atmosphere of solid oxide fuel cell. Journal of Power Sources, 2017, 360, 488-494.	7.8	7
18	Redox stability of La0.2Sr0.7Ti0.9Ni0.1O3-δ (LSTN)-Gd0.2Ce0.8O2-δ (GDC) composite anode. International Journal of Hydrogen Energy, 2017, 42, 28559-28566.	7.1	4

GYEONG MAN CHOI

#	Article	IF	CITATIONS
19	Effect of Gd-doped ceria interlayer on the stability of solid oxide electrolysis cell. Solid State Ionics, 2016, 295, 25-31.	2.7	13
20	Polarization and stability of La2NiO4+Î′ in comparison with La0.6Sr0.4Co0.2Fe0.8O3ⴴδ as air electrode of solid oxide electrolysis cell. International Journal of Hydrogen Energy, 2016, 41, 14498-14506.	7.1	40
21	Micro solid oxide fuel cell fabricated on porous stainless steel: a new strategy for enhanced thermal cycling ability. Scientific Reports, 2016, 6, 22443.	3.3	35
22	Stainless steel-supported solid oxide fuel cell with La0.2Sr0.8Ti0.9Ni0.1O3â^î/yttria-stabilized zirconia composite anode. Journal of Power Sources, 2016, 324, 288-293.	7.8	36
23	Flexible solid oxide fuel cells supported on thin and porous metal. International Journal of Hydrogen Energy, 2016, 41, 9577-9584.	7.1	25
24	Y0.08Sr0.88TiO3–CeO2 composite as a diffusion barrier layer for stainless-steel supported solid oxide fuel cell. Journal of Power Sources, 2016, 307, 385-390.	7.8	13
25	Effects of Fabrication Conditions on the Crystallinity, Barium Deficiency, and Conductivity of BaZr _{0.8} Y _{0.2} O _{3–} <i>_Î</i> Films Grown by Pulsed Laser Deposition. Fuel Cells, 2015, 15, 408-415.	2.4	14
26	Low-temperature fabrication of protonic ceramic fuel cells with BaZr0.8Y0.2O3â^`î´ electrolytes coated by aerosol deposition method. International Journal of Hydrogen Energy, 2015, 40, 2775-2784.	7.1	38
27	Effect of anode firing on the performance of lanthanum and nickel co-doped SrTiO3 (La0.2Sr0.8Ti0.9Ni0.1O3â^îî) anode of solid oxide fuel cell. Journal of Power Sources, 2015, 293, 684-691.	7.8	28
28	Phase stability and oxygen non-stoichiometry of Gd-doped ceria during sintering in reducing atmosphere. Journal of Electroceramics, 2015, 35, 68-74.	2.0	6
29	Novel modification of anode microstructure for proton-conducting solid oxide fuel cells with BaZr0.8Y0.2O3â~δ electrolytes. Journal of Power Sources, 2015, 285, 431-438.	7.8	22
30	Effect of Ce 0.43 Zr 0.43 Gd 0.1 Y 0.04 O 2â^'δ contact layer on stability of interface between GDC interlayer and YSZ electrolyte in solid oxide electrolysis cell. Journal of Power Sources, 2015, 284, 617-622.	7.8	23
31	Electrochemical performance and stability of La0.2Sr0.8Ti0.9Ni0.1O3-δ and La0.2Sr0.8Ti0.9Ni0.1O3-δ - Gd0.2Ce0.8O2-δ anode with anode interlayer in H2 and CH4. Electrochimica Acta, 2015, 182, 39-46.	5.2	19
32	Switchable Photovoltaic Effects in Hexagonal Manganite Thin Films Having Narrow Band Gaps. Chemistry of Materials, 2015, 27, 7425-7432.	6.7	67
33	A novel solid oxide electrolysis cell (SOEC) to separate anodic from cathodic polarization under high electrolysis current. International Journal of Hydrogen Energy, 2015, 40, 9032-9038.	7.1	29
34	Stability of LSCF electrode with GDC interlayer in YSZ-based solid oxide electrolysis cell. Solid State lonics, 2014, 262, 303-306.	2.7	81
35	Electrical conductivity of Gd-doped ceria film at low temperatures (300–500 °C). Solid State Ionics, 2014, 262, 411-415.	2.7	12
36	Ex-solution of Ni nanoparticles in a La0.2Sr0.8Ti1â^'xNixO3â^'δ alternative anode for solid oxide fuel cell. Solid State Ionics, 2014, 262, 345-348.	2.7	47

#	Article	IF	CITATIONS
37	Micro-solid oxide fuel cell supported on a porous metallic Ni/stainless-steel bi-layer. Journal of Power Sources, 2014, 249, 79-83.	7.8	15
38	Acceptor-doped ceria deposited on a porous Ni film as a possible micro-SOFC electrolyte. Journal of Electroceramics, 2013, 31, 238-244.	2.0	4
39	Electrical conductivity of Gd-doped ceria film fabricated by aerosol deposition method. Solid State lonics, 2013, 236, 16-21.	2.7	27
40	Enhanced power density of metal-supported solid oxide fuel cell with a two-step firing process. Solid State Ionics, 2011, 192, 519-522.	2.7	16
41	GdBaCo2O5+x cathode for anode-supported ceria SOFCs. Solid State Ionics, 2011, 192, 527-530.	2.7	16
42	Effects of anode firing temperature on the performance of the lanthanum-gallate thick-film-supported SOFC. Solid State Ionics, 2011, 192, 523-526.	2.7	8
43	Oxygen permeation of BSCF membrane with varying thickness and surface coating. Journal of Membrane Science, 2010, 346, 353-360.	8.2	96
44	Effect of electrolyte thickness on the performance of anode-supported ceria cells. Solid State Ionics, 2010, 181, 1702-1706.	2.7	25
45	Rapid Thermal-Cycling Test Using Thick-Film Electrolyte-Supported Solid Oxide Fuel Cells. Electrochemical and Solid-State Letters, 2010, 13, B17.	2.2	3
46	Effect of Ni doping on the phase stability and conductivity of scandia-stabilized zirconia. Solid State Ionics, 2009, 180, 252-256.	2.7	16
47	The effects of LSM coating on 444 stainless steel as SOFC interconnect. Journal of Electroceramics, 2009, 22, 67-72.	2.0	12
48	Fabrication and characterization of Ni-supported solid oxide fuel cell. Solid State Ionics, 2009, 180, 792-795.	2.7	28
49	Micro-solid oxide fuel cell using thick-film ceria. Solid State Ionics, 2009, 180, 839-842.	2.7	24
50	Performance of La-doped strontium titanate (LST) anode on LaGaO3-based SOFC. Solid State Ionics, 2009, 180, 867-871.	2.7	78
51	The effect of alumina and Cu addition on the electrical properties and the SOFC performance of Gd-doped CeO2 electrolyte. Solid State Ionics, 2009, 180, 886-890.	2.7	38
52	Effect of milling methods on performance of Ni–Y2O3-stabilized ZrO2 anode for solid oxide fuel cell. Journal of Power Sources, 2008, 176, 96-101.	7.8	64
53	Thick-film electrolyte (thickness <20μm)-supported solid oxide fuel cells. Journal of Power Sources, 2008, 180, 195-198.	7.8	27
54	Zirconia as a high temperature oxygen-permeating membrane: The effect of GDC and LaCrO3 surface coating. Solid State Ionics, 2008, 179, 1372-1376.	2.7	2

#	Article	IF	CITATIONS
55	Electrical conductivity of the Al-stabilized La2/3TiO3. Journal of Electroceramics, 2008, 20, 127-132.	2.0	2
56	Electrical conductivity of scandia-stabilized zirconia thin film. Solid State Ionics, 2008, 179, 1209-1213.	2.7	20
57	Electrochemical Deoxidation of Molten Steel with Application of an Oxygen Permeable Membrane. ISIJ International, 2007, 47, 689-698.	1.4	11
58	Cathodic overpotential of La0.6Sr0.4CoO3 and its composite cathodes LSC–LSGM on LaGaO3-based fuel cell. Journal of the European Ceramic Society, 2007, 27, 4211-4214.	5.7	7
59	Oxygen-permeating zirconia membrane: The effect of thickness and surface coating. Journal of the European Ceramic Society, 2007, 27, 4219-4222.	5.7	4
60	Oxygen permeation characteristics of zirconia with surface modification. Solid State Ionics, 2006, 177, 2261-2267.	2.7	11
61	The effect of Co addition on the electrical conductivity of Sr- and Mg-doped LaAlO3. Journal of Electroceramics, 2006, 17, 787-791.	2.0	4
62	Impedance spectroscopy of acceptor-doped CaZrO3 with cation nonstoichiometry. Journal of Electroceramics, 2006, 17, 1091-1095.	2.0	8
63	Oxygen exchange and transport properties of yttria-stabilized zirconia coated with LaCrO3. Journal of Electroceramics, 2006, 17, 781-786.	2.0	5
64	The effect of alumina addition on the electrical conductivity of Gd-doped ceria. Journal of Electroceramics, 2006, 17, 793-798.	2.0	25
65	The effect of transition-metal addition on the non-equilibrium E.M.Ftype gas sensor. Journal of Electroceramics, 2006, 17, 1019-1022.	2.0	3
66	The effect of cation nonstoichiometry on the electrical conductivity of acceptor-doped CaZrO3. Solid State Ionics, 2006, 177, 3099-3103.	2.7	22
67	The effect of cation nonstoichiometry on the electrical conductivity of CaZrO3. Journal of the European Ceramic Society, 2005, 25, 2609-2612.	5.7	26
68	The effect of reduction atmosphere on the LaGaO3-based solid oxide fuel cell. Journal of the European Ceramic Society, 2005, 25, 2655-2659.	5.7	4
69	The effect of mixed conductivity on the cathodic overpotential of LaGaO3-based fuel cell. Solid State Ionics, 2004, 175, 145-149.	2.7	13
70	Selective Gas Detection of SnO2-TiO2 Gas Sensors. Journal of Electroceramics, 2004, 13, 707-713.	2.0	37
71	Oxygen permeability of gadolinium-doped ceria at high temperature. Journal of the European Ceramic Society, 2004, 24, 1313-1317.	5.7	30
72	Oxygen permeation in Sr- and Mg-doped LaAlO3 and Gd-doped CeO2 at high temperature. Solid State Ionics, 2004, 175, 399-403.	2.7	11

#	Article	IF	CITATIONS
73	Cathodic properties of La0.9Sr0.1MnO3 electrode for fuel cells based on LaGaO3 solid electrolyte. Journal of the European Ceramic Society, 2004, 24, 1359-1363.	5.7	24
74	The CO and H2 gas selectivity of CuO-doped SnO2–ZnO composite gas sensor. Sensors and Actuators B: Chemical, 2002, 87, 464-470.	7.8	132
75	Partial electronic conductivity of Sr and Mg doped LaGaO3. Solid State Ionics, 2002, 154-155, 481-486.	2.7	22
76	Phase characterization and electrical conductivity of LaSr(GaMg)1â^'xMnxO3 system. Solid State Ionics, 2002, 148, 557-565.	2.7	31
77	Selective CO Gas Detection of Zn2SnO4 Gas Sensor. , 2002, 8, 249-255.		52
78	Electrical Conductivity of Ionic and Electronic Mixture. Materials Research Society Symposia Proceedings, 2001, 699, 961.	0.1	0
79	Non-Ohmic Current-Voltage and Impedance Characteristics of Electroadsorptive Zn[sub 2]SnO[sub 4]. Journal of the Electrochemical Society, 2001, 148, G307.	2.9	15
80	THE EFFECT OF SINTERING ON THE ELECTRICAL CONDUCTIVITY OF LITHIUM LANTHANUM TITANATES. , 2000, , .		0
81	Electrical conductivity of CeO2-doped YSZ. Solid State Ionics, 2000, 135, 653-661.	2.7	44
82	Mixed ionic and electronic conductivity of [(ZrO2)0.92(Y2O3)0.08]1â^'y·(MnO1.5)y. Solid State Ionics, 2000, 130, 157-168.	2.7	52
83	PHASE CHARACTERIZATION AND ELECTRICAL PROPERTIES OF LSM-LSGM SYSTEM. , 2000, , .		0
84	Mixed Ionic and Electronic Conduction in YSZâ€NiO Composite. Journal of the Electrochemical Society, 1999, 146, 883-889.	2.9	37
85	Title is missing!. , 1999, 3, 361-369.		84
86	Impedance Spectra for a 2-D Conductor-Insulator Composite by Computer Simulation. , 1998, 2, 57-66.		3
87	Composition Dependence of the Electrical Conductivity of ZnO(<i>n</i>)–CuO(<i>p</i>) Ceramic Composite. Journal of the American Ceramic Society, 1998, 81, 695-699.	3.8	51
88	Humidity Response Characteristics of Barium Titanate. Journal of the American Ceramic Society, 1993, 76, 766-768.	3.8	46
89	Electrical Conduction in Aluminum Nitride. Journal of the American Ceramic Society, 1993, 76, 957-960.	3.8	27
90	Effects of Dopants on the Complex Impedance and Dielectric Properties of Aluminum Nitride. Journal of the American Ceramic Society, 1992, 75, 3145-3148.	3.8	10

#	Article	IF	CITATIONS
91	Defect Structure and Electrical Properties of Single-Crystal Ba0.03Sr0.97TiO3. Journal of the American Ceramic Society, 1988, 71, 201-205.	3.8	130